Vector Channels for Smart Antennas—Measurements, Statistical Modeling, and Directional Properties in Outdoor Environments

Adnan Kavak, *Student Member, IEEE*, Murat Torlak, *Member, IEEE*, Wolfhard J. Vogel, *Fellow, IEEE*, and Guanghan Xu, *Member, IEEE*

***Abstract*—In wireless communications, smart antenna systems that employ antenna arrays coupled with adaptive signal-processing techniques at the basestation improve capacity, coverage, and trunking efficiency. However, design and performance analysis of smart antenna systems strongly depend on channel propagation characteristics of signals present at the antenna array, the so-called *vector channels*. Here, variation of narrow-band vector channels (*spatial signatures*) due to a moving terminal is studied in typical suburban settings. Vector channel measurements are taken using a real-time smart antenna system with a uniform circular array at the basestation and a mobile transmitter at several locations. Two different wireless scenarios, namely, pedestrian and car mobile, are implemented to emulate the random movement of the mobile user. In each scenario, the mobile transmitter locations are chosen so that there exists line-of-sight (LOS), nonline-of-sight (NOLOS), or both LOS and NOLOS (mixed) propagation to the basestation. We find that in all cases, the Beta distribution can be used to empirically represent the spatial signature correlations and that large spatial diversity exists in NOLOS cases compared to LOS cases. Also, direction-of-arrivals mostly do not change much with movement in a suburban environment.**

***Index Terms*—Direction-of-arrivals, line-of-sight, narrow-band channel, nonline-of-sight, probability distribution, propagation modeling, smart antennas, space diversity, spatial signature, vector channels.**

I. Introduction

As THE demands for higher capacity and higher data rates are increasing, smart antenna systems that use multiple antennas (antenna arrays) at the basestation along with advanced space–time signal processing algorithms are becoming a promising technology in wireless communication systems [1]. By exploiting the spatial dimension in signal processing, smart antenna systems allow multiple users to transmit co-channel signals in the same time slot and frequency band and mitigate interference, thereby improving capacity and extending the range in wireless systems. Interference rejection or signal-to-interference-plus-noise-ratio (SINR) improvement capability of an antenna array is, however, strongly affected by the spatial (array geometry, antenna element characteristics, direction-of-arrivals (DOA's), signal polarization) and temporal (time-of-arrivals, transmitted waveforms) channel propagation characteristics. A thorough understanding of these factors, therefore, is necessary to fully exploit smart antenna systems.

The channel propagation characteristics of smart antenna systems can be described by a vector quantity usually called *vector channels* because a vector of signal samples is received/transmitted by the antenna array at each instant of time. Accurate vector channel models are of great importance for the simulation, performance analysis, and optimization of smart antenna systems. To develop an accurate vector channel model, it is paramount to perform extensive measurements in realistic wireless environments, taking into account propagation environment dynamics (movement, basestation antenna deployment, etc.).

Previous work on vector channel measurements [2] using a real-time smart antenna system explored the effects of movement in a deterministic or semideterministic way such as relative angle and amplitude change of spatial signatures and multipath fading parameters. However, for the cell-site design of basestation antenna arrays, statistical description of spatial signature variation may provide more insightful information than a deterministic description. Knowledge of the statistics associated with spatial signatures for a given environment helps system engineers determine two main approaches for the operation of smart antennas. These approaches include beamforming techniques in selecting intended user (or canceling interferers) in downlink and antenna array diversity gain in combating multipath fading in uplink.

For single antenna systems, cumulative distributions of fade duration statistics have been studied in depth [3],[1] [4]. In this paper, we will consider a similar analysis for the variation of spatial signatures of smart antenna systems. We aim to investigate how we can statistically describe and model the variations of spatial signature correlations observed in measurements taken in typical suburban settings. The measurements were performed using a real-time smart antenna system with a uniform circular array at the basestation. A mobile transmitter was used with pedestrian and car-mobile scenarios for which measurements were taken at three different mobile locations, i.e., representing a typical line-of-sight (LOS) only, a non-line-of-sight (NOLOS) only, and mixed (both LOS and NOLOS) propagation environments.

Manuscript received October 11, 1999. This work was supported in part by Southwestern Bell Technology Resources Inc. and by Samsung Telecommunications America Inc. An earlier version of this paper was presented in part at the 1999 IEEE Radio and Wireless Conference.

A. Kavak, W. J. Vogel, and G. Xu are with the Department of Electrical and Computer Engineering, The University of Texas at Austin, Austin, TX 78712 USA.

M. Torlak is with the Department of Electrical Engineering, The University of Texas at Dallas, Richardson, TX 75083 USA.

Publisher Item Identifier S 0018-9480(00)05031-6.

[1][Online]. Available: http://www.utexas.edu/research/mopro/

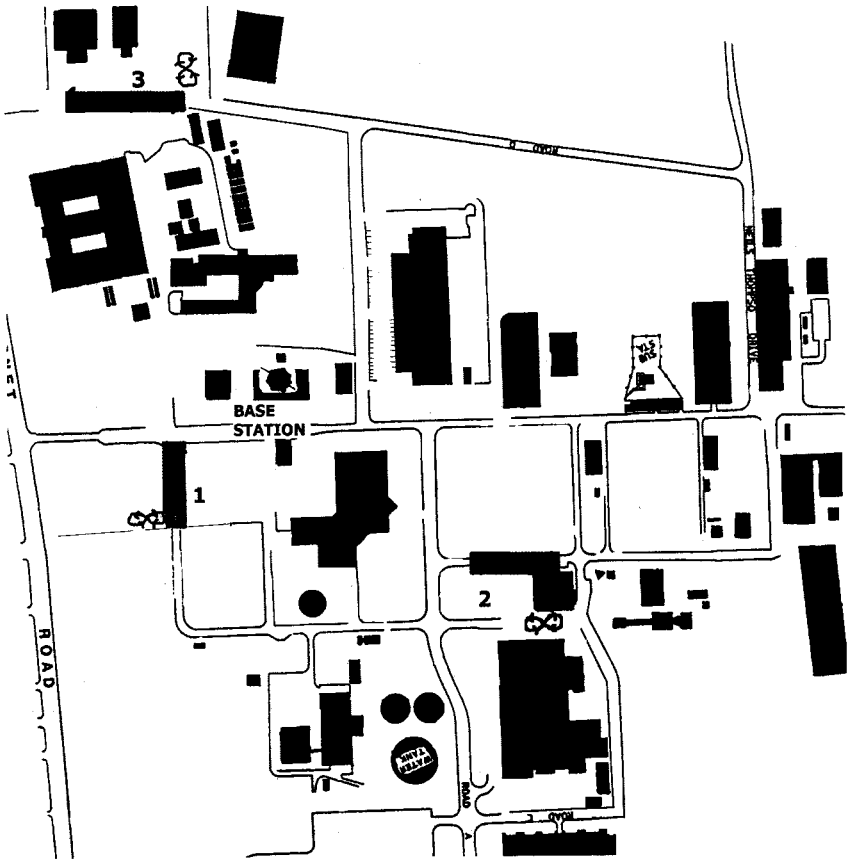

Fig. 1. Measurement environment: research campus of The University of Texas at Austin.

The paper is organized as follows. Section II briefly explains the vector channel concept. Section III introduces the measurement campaign. Section IV describes our real-time smart antenna test bed developed at The University of Texas at Austin that is used for taking vector channel measurements. Statistical analysis and modeling of spatial signature correlations are presented in Section V. Measurement results regarding the variation of DOA's are discussed in Section VI. Finally, the paper is concluded in Section VII.

II. Vector Channel Concept

Consider L multipath signals originated from a mobile impinging upon an M-element uniform circular array (which is practical for real wireless scenarios, wherein a 360° field of view is required). The signal wavefront of path l with carrier frequency f_c is then given by

$$r_l(t) = s_l(t)e^{j2\pi f_c t}. \tag{1}$$

The received signal $x_i(t)$ at the ith antenna element due to signal wavefront $r_l(t)$ will be

$$x_i(t) = r_l(t - \tau_{l,i}) = s_l(t - \tau_{l,i})e^{j2\pi f_c(t-\tau_{l,i})} \tag{2}$$

Fig. 2. Smart antenna basestation tower.

where $\tau_{l,i}$ is the time delay experienced by the received signal at the ith antenna element with respect to the reference signal wavefront usually at the first antenna element. If $s_l(t)$ is slowly varying compared to the carrier ($B \ll f_c$) and its inverse bandwidth is much larger than the time interval required for the wavefront to propagate across the array ($\tau_{l,M} \ll B^{-1}$), then the

TABLE I
DESCRIPTION OF EXPERIMENTAL LOCATIONS

Location	*Scenario*	*Propagation Path*	*Mobile Range*
1	Pedestrian	LOS	170 m.
2	Pedestrian	NOLOS	270 m.
3	Pedestrian	NOLOS	320 m.
1	Car Mobile	LOS	150-170 m.
2	Car Mobile	LOS+NOLOS	250-270 m.
3	Car Mobile	NOLOS	300-320 m.

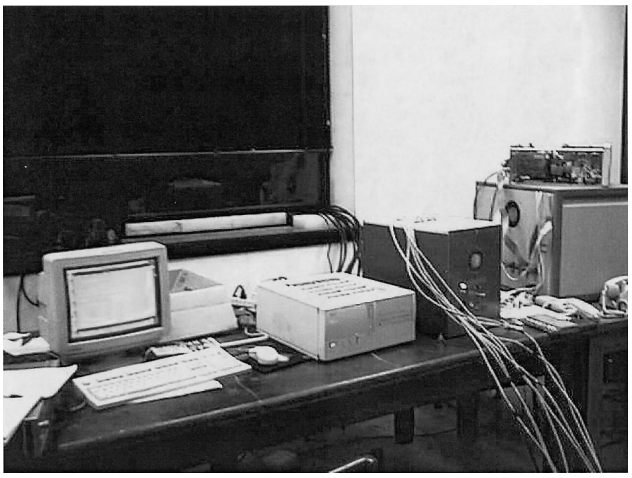

Fig. 3. Smart antenna test bed.

narrow-band assumption applies and $s_l(t-\tau_{l,i}) \approx s_l(t)$. Substituting this into (2) yields

$$x_i(t) = e^{-j2\pi f_c \tau_{l,i}} s_l(t) e^{j2\pi f_c t} = e^{-j2\pi f_c \tau_{l,i}} r_l(t). \quad (3)$$

Thus, for an M-element array, the snapshot vector model of the received signal due to multipath wavefront $r_l(t)$ can then be obtained as

$$\mathbf{x}(t) = \boldsymbol{\vartheta}(\theta_l) r_l(t) + \mathbf{n}(t) \quad (4)$$

where

$$\boldsymbol{\vartheta}(\theta_l) = \left[e^{-j2\pi f_c \tau_{l,1}}, \cdots, e^{-j2\pi f_c \tau_{l,M}}\right]^T \quad (5)$$

is a *steering vector or array response vector* to the signal wavefront arriving from angle θ_l, and $\mathbf{n}(t)$ is an $Mx1$ spatially white additive noise vector.

Equation (4) represents the received signal vector with respect to the signal wavefront. Since the signal wavefront $r_l(t)$ will be an attenuated and delayed version of the original transmitted baseband signal $s(t)$, then

$$r_l(t) = \alpha_l(t) e^{j\varphi_l(t)} s\big(t - \Delta_l(t)\big) e^{j2\pi f_c t}$$

where $\alpha_l(t)$ and $\varphi_l(t)$ are amplitude and phase of the complex path attenuation, respectively, and Δ_l is the multipath delay. If the multipath delay is negligible, i.e., $\max\{\Delta_l\} \ll B^{-1}$, then $s(t-\Delta_l(t)) \approx s(t)$. By summing up the $L(t)$ multipath components and including large-scale effects Γ_l (ground specular reflection, path loss), we can rewrite the received signal in (4) as [5]

$$\mathbf{x}(t) = \sum_{l=1}^{L(t)} \Gamma_l \alpha_l(t) e^{j\varphi_l(t)} \boldsymbol{\vartheta}(\theta_l) s\big(t - \Delta_l(t)\big) + \mathbf{n}(t) \quad (6)$$

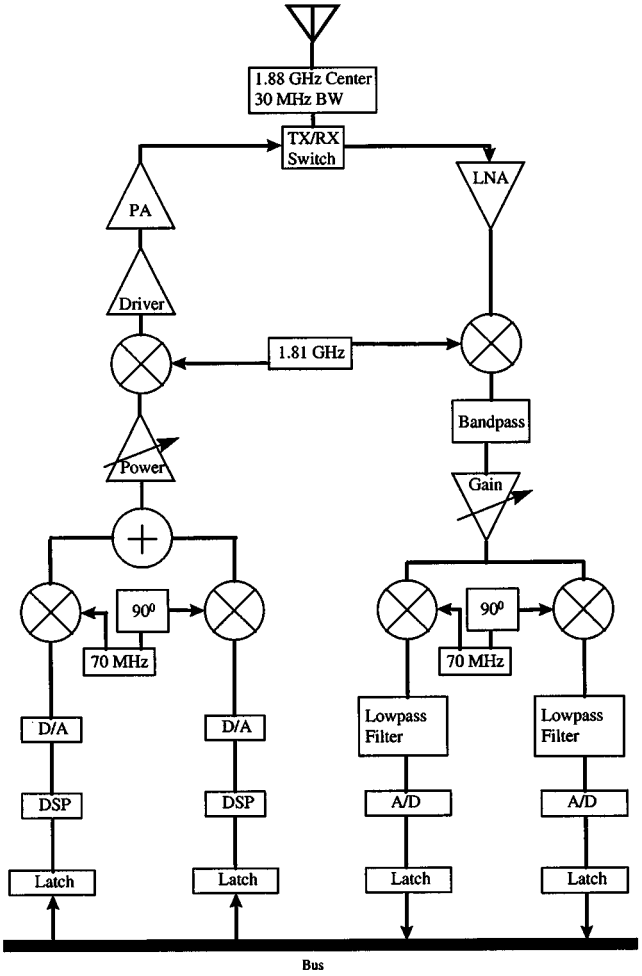

Fig. 4. Schematic of one T/R unit of the smart antenna test bed.

TABLE II
BEST-FIT PARAMETERS, RMSE'S AND CHI-SQUARE TEST STATISTICS FOR THE MODEL ESTIMATE OF SPATIAL SIGNATURE CORRELATIONS IN PEDESTRIAN AND CAR-MOBILE SCENARIOS

	Pedestrian Scenarios			*Car Mobile Scenarios*		
	Loc.1	*Loc.2*	*Loc.3*	*Loc.1*	*Loc.2*	*Loc.3*
μ	0.99	0.95	0.78	0.90	0.79	0.59
σ	0.007	0.04	0.17	0.08	0.15	0.25
ψ	166.66	26.74	2.93	9.1	4.03	0.65
β	0.33	0.56	0.08	0.004	0.35	0.14
$S^e_{pdf}(\%)$	0.34	0.24	0.26	0.32	0.20	0.20
$S^e_{ccdf}(\%)$	1.56	1.00	3.94	4.32	3.33	1.25
Q	2.88	0.71	8.63	15.47	7.93	1.79
$\chi^2_{0.95;K}$	22.36	19.68	23.68	19.68	23.68	25.00
K	13	11	13	11	14	15

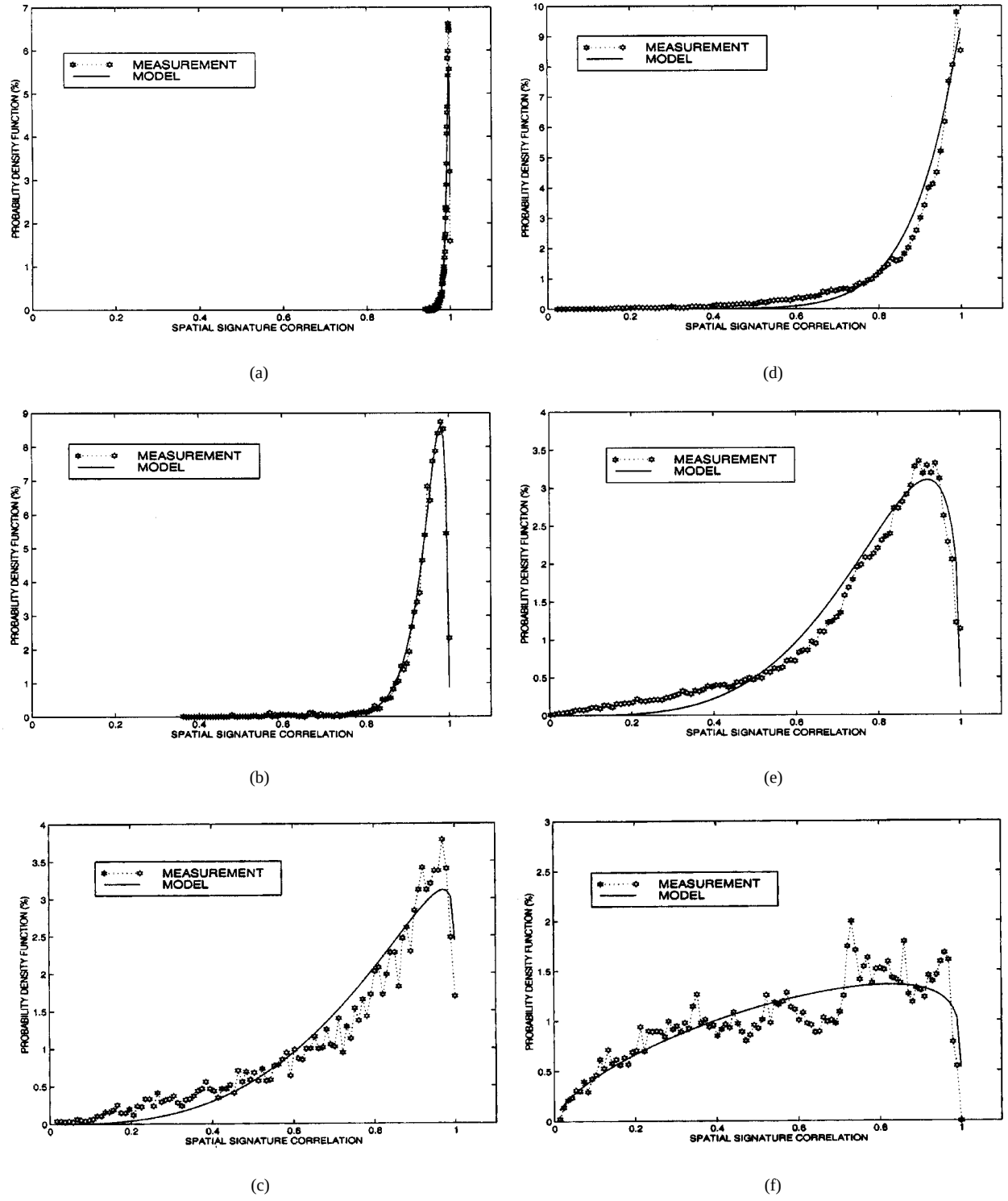

Fig. 5. Measured and modeled PDF's of spatial signature correlations for pedestrian and car-mobile scenarios in a suburban environment. (a) Loc.1—pedestrian. (b) Loc.2—pedestrian. (c) Loc.3—pedestrain. (d) Loc.1—car mobile. (e) Loc.2—car mobile. (f) Loc.3—car mobile.

where the narrow-band vector channel given by

$$\mathbf{a}(t) = \sum_{l=0}^{L(t)-1} \Gamma_l \alpha_l(t) e^{j\varphi_l(t)} \vartheta(\theta_l) \tag{7}$$

is referred to as the *spatial signature*, and is the objective of our measurements.

III. Measurement Campaigns

The vector channel measurements were performed in the suburban environment on the grounds of the Pickle Research Campus, The University of Texas at Austin (Fig. 1). The measurement system was comprised of a basestation receiver and mobile transmitter. At the basestation receiver site was a real-time smart antenna test bed with an antenna array arranged in a seven-element uniform circular pattern with a radius of

10 cm. The elements of the array were vertically polarized collinear dipole antennas with 2-dBi gain. The antenna array platform was placed at the top of a 20-m telescoping tower, as shown in Fig. 2.

At the mobile transmitter site was an omnidirectional vertically polarized $\lambda/2$ dipole antenna excited by an HP 8662A signal generator. The test signal transmitted was an unmodulated sine wave carrier at a frequency of 1880.25 MHz. We studied two different wireless scenarios, namely, pedestrian and car mobile. Three different mobile locations were chosen for each scenario so that typical LOS propagation, NOLOS propagation, or a mixture of LOS and NOLOS propagation to the basestation existed as summarized in Table I.

In the pedestrian scenarios, the mobile transmitter antenna attached to a 1.5-m-tall wooden stand was moved within a 3-m diagonal square area in order to emulate the random positions of a mobile user. Data were collected for a total of 40 approximately equispaced discrete positions along a figure-eight-shaped path (see Fig. 1) in each location. Subsequent to the pedestrian measurements, the experimental procedures were repeated on a different day for the car-mobile scenarios at approximately the same locations as depicted in Fig. 1. In this case, the transmitter antenna was mounted on a car that was driven at an average speed of 30 m/h (13.4 m/s). At each location, about a total of ten car runs (five each in forward and reverse directions) were performed, thereby repeatedly covering a range of approximately 20 m. During each car run, we collected sets of three consecutive data snapshots with the test bed, each with 3-ms duration and approximately equidistant over the run. Then spatial signatures were estimated from 0.3-ms data, providing ten spatial signatures per snapshot.

The average rooftop height of buildings, the major potential scattering sources in the measurement environment, was 10 m. Surrounding the basestation were a few structures and trees, which did not contribute any strong multipath signal arriving at the antenna array because the basestation tower was fully deployed and higher than its surrounding scatterers. In the NOLOS scenarios, there were both local scatterers in the vicinity of the mobile and remote scatterers with respect to both the mobile and basestation.

IV. Real-Time Smart Antenna Test-Bed Description

The RF signals received by the antenna array elements are fed to the eight-channel smart antenna test bed shown in Fig. 3. Since a seven-element array is used, one channel of the test bed is idled. The test bed consists of personal computer with an EZ-ICE in-circuit emulator, four transmit/receive (T/R) boards, and a digital signal processor board with two Analog Devices SHARC chips. Each T/R board has two T/R channels. The EZ-ICE emulator controls the operation of the SHARC chips, each connected to four T/R channels. A block diagram of one T/R channel is depicted in Fig. 4. Since we use only the receive channels for the measurements, we will restrict the explanation to the receive part of the board. The received RF signals at a frequency of 1880.25 MHz are mixed down with a 1810.25-MHz reference to generate a 70-MHz IF signal. Then,

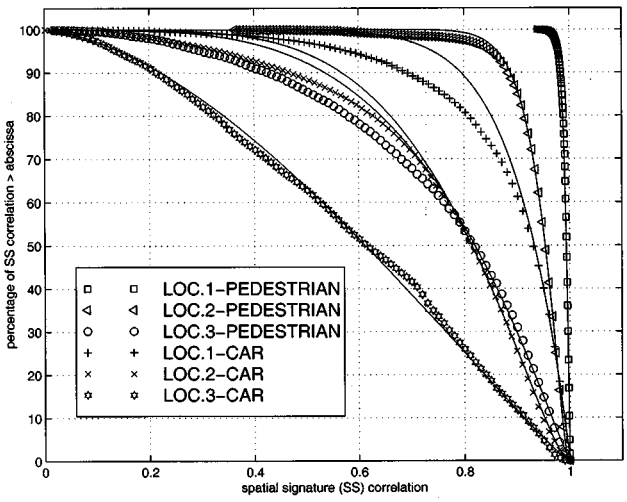

Fig. 6. Measured and modeled CCDF's of spatial signature correlations for pedestrian and car-mobile scenarios in a suburban environment.

the in-phase (I) and quadrature (Q) baseband signals are generated by multiplying the IF signal with an I-Q pair of 70-MHz frequency, low-pass filtered and sampled at 3.072 Msamples/s per channel. The samples are digitized, latched, and put onto the system bus. The data is then transferred to the controlling computer for analysis. A data snapshot of 7×9600 complex valued samples can be collected in approximately 3 ms.

V. Statistical Analysis and Modeling of Spatial Signature Variations

The performance and interference rejection capability of smart antenna systems depend on the spatial signatures of the mobile users. In a dynamical multipath propagation environment, where there is relative motion between the mobile user and the basestation, spatial signatures vary randomly and, therefore, their variation, must be analyzed in a statistical sense. For each location in pedestrian and car-mobile scenarios, the received data snapshots are processed to estimate the spatial signatures $a(t)$ defined in (7). We quantify the variation of spatial signatures by their correlations given by

$$\rho_{i,j} = \frac{a_i^H a_j}{||a_i||\,||a_j||}, \qquad i \neq j \tag{8}$$

where a_i and a_j are the spatial signatures at ith and jth mobile positions, respectively, and H is the Hermitian transpose operator. Correlation of spatial signatures is a useful measure to determine the update rate of spatial signatures and the level of spatial diversity in the environment. For instance, if the correlations remain high (e.g., 90%) for a large percentage of time during which the mobile user moves, we do not need to update spatial signatures very often. In this case, it is conceivable to use uplink spatial signatures for downlink transmission in time-division-duplex (TDD) schemes [6]. The high correlation, however, implies that there is little diversity in the environment for space-division multiple-access (SDMA) applications [1] and, therefore, in the uplink process, we cannot effectively benefit from antenna array diversity gain to separate SDMA users.

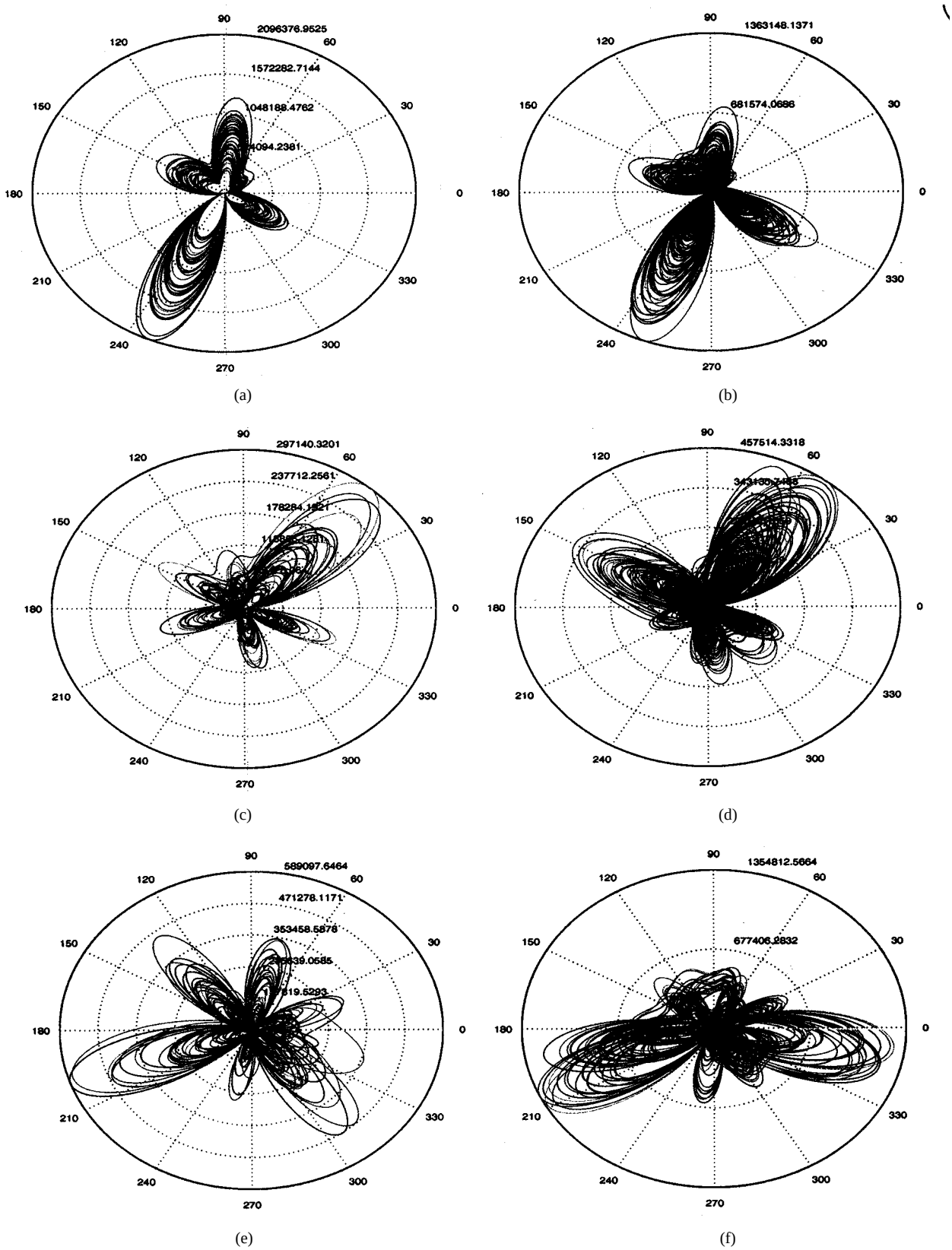

Fig. 7. DOA Estimates. (a) Loc.1—pedestrian. (b) Loc.1—car mobile. (c) Loc.2—pedestrain. (d) Loc.2—car mobile. (e) Loc.3—pedestrain. (f) Loc.3—car mobile.

To develop a statistical model of spatial signatures, a sufficiently large number of correlations is produced by calculating $\rho_{i,j}$ values in (8) between any spatial signature pairs for each location, i.e., about $C\binom{40}{2}$ and $C\binom{250}{2}$ possible $\rho_{i,j}$ values for pedestrian and car-mobile scenarios, respectively. We then obtained the measured probability distribution functions

(PDF's) of $\rho_{i,j}$. By nonlinear optimization, an empirical model that overall best fits the measured family of PDF's is found to be the Beta function [7] given by

$$f(\rho|\psi,\beta)=\frac{\Gamma(\psi+\beta+2)}{\Gamma(\psi+1)\Gamma(\beta+1)}\rho^{\psi}(1-\rho)^{\beta},\qquad 0\le\rho\le 1;\quad \psi>-1;\quad \beta>-1 \tag{9}$$

where $\Gamma(\cdot)$ is the Gamma function defined as

$$\Gamma(t)=\int_0^{\infty} x^{t-1}e^{-x}\,dx=(t-1)!.$$

The resultant best-fit model parameters (ψ, β), mean (μ), and standard deviation (σ) are summarized in Table II.

Measured and modeled PDF's of spatial signature correlations are shown in Fig. 5 for pedestrian [see Fig. 5(a), (b), and (c)] and car-mobile [see Fig. 5(d), (e), and (f)] scenarios. It is seen that the distributions are skewed to the left-hand side for all locations. In Fig. 6 are plotted complementary cumulative density functions (CCDF's) of spatial signature correlations derived from the PDF's. Except at location 3 of pedestrian and at locations 1 and 2 of car-mobile cases, there is a good agreement between measured and modeled CCDF's. We notice that the PDF's stretch out to low correlation levels with changing mobile user location from an LOS to NOLOS propagation environment, i.e., the distributions become less skewed. In each scenario, we also observe that ψ and μ values decrease and the convexity of CCDF curves reduces. This is because in NOLOS propagation, spatial signatures considerably change and become less correlated due to varying complex path attenuation α, φ [see (7)] of multipath signals with even small movements. The results also suggest that there exists large spatial diversity in NOLOS environments compared to LOS environments.

A. Testing Model Accuracy

Having calculated the model parameters, it is of interest to determine how closely the theoretical model fits to measured distribution of spatial signature correlations. The standard error of regression or root-mean-square error (RMSE), which is defined as $S^e=\sqrt{\Sigma E_i^2/n-m}$, where E_i is the residual, n is the number of data bins, and m is the number of coefficients fitted, provides one sort of information about the accuracy of the model. S^e values for both PDF and CCDF estimates are listed in Table II. The worst-case RMSE (4.32%) is observed when deriving the CCDF estimate for location 1 of the car-mobile scenario. In estimating PDF's, the RMSE values for all locations are found to be smaller than 0.34%. RMSE criteria may not be a very reliable method for testing the model accuracy [8] because it represents a type of "average" residual. Therefore, we carried out the chi-square goodness-of-fit test, in which we first calculated the quantity Q defined by

$$Q=\sum_{i=1}^{K+1}\frac{(\text{measured dist.}-\text{theoretical dist.})^2}{\text{theoretical dist.}} \tag{10}$$

where K represents the *degrees of freedom*. In evaluating (10), it was ensured that probabilities of each bin along the abscissa are larger than or equal to 5%. Next, we compared Q with the chi-square distribution $\chi^2_{0.95;K}$ with K degrees of freedom and obtained $Q<\chi^2_{0.95;K}$ for all locations, as summarized in the last three rows of Table II. Thus, both RMSE criteria and the chi-square test indicate that the Beta function in (9) is capable of representing spatial signature variations in typical suburban settings. The empirical regression model proposed here has the advantage of being based on actual data and, hence, it may be employed to predict spatial signature correlations and to evaluate the performance of smart antenna systems in similar types of propagation environments.

VI. Variation of DOA's

In the previous section, we analyzed the relative change of spatial signatures due to a moving mobile in a typical suburban environment. To explore channel dynamics leading to spatial signature variations, we also examine the variation of DOA's of multipath components. DOA's estimated via the classical beamforming method [9] are plotted in Fig. 7. DOA variations shown in the left-hand-side column are for pedestrian scenarios and in the right-hand-side column for car-mobile scenarios. In all cases, we note that the DOA's are clustered around a few angles. For all locations in the pedestrian scenario and location 1 in the car-mobile scenario, the DOA's do not change much. However, we observe that the main DOA's slightly change for locations 2 and 3 in the car-mobile scenario, where the relative position of any scatterer changes quickly with the motion under NOLOS propagation condition. The stability of DOA's indicates that a significant contribution to spatial signature variation comes from varying path lengths or reflection coefficient changes of scatterer's surfaces.

VII. Conclusion

We have presented measurement and statistical modeling results of *narrow-band vector channel* or *spatial signature* variations for randomly moving mobile user scenarios (pedestrian and car mobile) in a suburban environment. A 1.8-GHz real-time smart antenna test bed with a uniform circular array at the basestation was used to perform the measurements. Three different mobile locations having typical LOS, NOLOS, and a mixture of LOS and NOLOS propagation to the basestation were chosen to take measurements. Statistical properties of the spatial signature correlations are explored under these wireless scenarios. It is observed that NOLOS propagation conditions exhibit lower spatial signature correlations than LOS propagation conditions. An empirical regression model (Beta distribution) for the PDF's of spatial signature correlations is proposed. Although there is no physical or analytical basis for the model, it may be used with a certain degree of confidence for the prediction of spatial signature variations in similar types of environments. It is also observed that DOA's, except for the NOLOS propagation in the car-mobile scenario, are not very variable.

References

[1] J. H. Winters, "Smart antennas for wireless systems," *IEEE Pers. Commun. Mag.*, vol. 5, no. 1, pp. 23–27, Feb. 1998.

[2] A. Kavak, W. Yang, and G. Xu, "Characterization of fast fading wireless vector channels," in *Proc. IEEE Asilomar Conf. Signals, Syst., Comput.*, Pacific Grove, CA, Nov. 1998, pp. 780–784.

[3] J. Goldhirsh and W. J. Vogel, *Handbook of Propagation Effects for Vehicular and Personal Mobile Satellite Systems*, 2nd ed. Pasadena, CA: Jet Propulsion Lab., 1998.
[4] J. D. Parsons, *The Mobile Radio Propagation Channel*. New York: Wiley, 1996.
[5] A. Paulraj and C. B. Papadias, "Space-time processing for wireless communications," *IEEE Signal Processing Mag.*, pp. 49–83, Nov. 1997.
[6] W. Yang, A. Kavak, S. Kim, G. Xu, and L. Hansen, "Evaluation of spatially selective receiving/transmission techniques for a smart antenna system operating at 1.8 GHz in nonstationary scenarios," in *Proc. IEEE Veh. Technol. Conf.*, Houston, TX, May 1999, pp. 862–866.
[7] M. H. DeGroot, *Probability and Statistics*. Reading, MA: Addison-Wesley, 1989.
[8] J. Fox, *Applied Regression Analysis, Linear Models, and Related Methods*. Beverly Hills, CA: Sage, 1997.
[9] H. Krim and M. Viberg, "Two decades of array signal processing research," *IEEE Signal Processing Mag.*, pp. 67–94, July 1996.

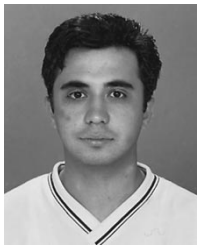

Adnan Kavak (S'96) was born on June 6, 1970, in Usak, Turkey. He received the B.Sc. degree in electrical engineering from the Middle East Technical University, Ankara, Turkey, in 1992, the M.S. degree in electrical engineering from The University of Texas at Austin, in 1996, and is currently working toward the Ph.D. degree in electrical engineering at The University of Texas at Austin.

From December 1992 to June 1994, he was a Satellite Control and Communications Engineer at the Turksat Satellite Control Center, Turk Telecom, Ankara, Turkey. His current research interests include channel propagation and smart antenna systems for wireless communications.

Murat Torlak (S'94–M'00) was born on August 12, 1971 in Konya, Turkey. He received the B.S. degree in electrical and electronics engineering from Hacettepe University, Ankara, Turkey, in 1992, and the M.S. and Ph.D. degrees in electrical engineering from The University of Texas at Austin, in 1995 and 1999, respectively.

In the Fall of 1999, he joined the Department of Electrical Engineering, The University of Texas at Dallas, where he is currently an Assistant Professor. His current research interests include hardware–software wireless system integration, software radios, and statistical signal processing.

Wolfhard J. Vogel (S'69–M'74–SM'90–F'94) studied electrical engineering at the Technical University of Berlin, Berlin, Germany, and received the Ph.D. degree in electrical engineering from The University of Texas at Austin.

He was Associate Director of the Electrical Engineering Research Laboratory (EERL), The University of Texas at Austin, until his recent retirement, and is currently a Research Scientist. Since 1974, he has had governmental and industrial support for performing satellite–Earth wave propagation research, emphasizing rain attenuation and depolarization effects at frequencies above 10 GHz and fading due to shadowing and multipath for land-mobile and personal communications from UHF to K-band. He also has guided vector channel propagation measurements made with The University of Texas "smart" antenna test bed.

Guanghan Xu (S'86–M'88) was born on November 10, 1962, in Shanghai, China. He received the B.S. degree (with honors) in biomedical engineering from Shanghai Jiao Tong University, Shanghai, China, in 1985, the M.S. degree in electrical engineering from Arizona State University, Tempe, in 1988, and the Ph.D. degree in electrical engineering from Stanford University, Stanford, CA, in 1991.

During the summer of 1989, he was a Research Fellow at the Institute of Robotics, Swiss Institute of Technology, Zurich, Switzerland. From 1990 to 1991, he was a General Electric Fellow of the Fellow–Mentor–Advisor Program at the Center of Integrated Systems, Stanford University. From 1991 to 1992, he was a Research Associate in the Department of Electrical Engineering, Stanford University, and a short-term Visiting Scientist at the Laboratory of Information and Decision Systems, Massachusetts Institute of Technology. In 1992, he joined the faculty of the Department of Electrical and Computer Engineering, The University of Texas at Austin, where he is currently an Associate Professor. He has worked in several areas, including signal processing, communications, numerical linear algebra, multivariate statistics, and semiconductor manufacturing. His current research interest is focused on smart antenna systems for wireless communications.

Dr. Xu is a member of Phi Kappa Phi and was the recipient of the 1995 National Science Foundation CAREER Award.